

Validation of a Biophysical Drug Absorption Model by the PATQSAR System[†]

MARIVAL BERMEJO, VIRGINIA MERINO, TERESA M. GARRIGUES, JOSE M. PLA DELFINA, ANTONIO MULET,[‡] PATRICK VIZET,^{§,||} GERARD TROUILLER,[§] AND CHRISTIANE MERCIER^{*,||}

Contribution from *Department of Pharmaceutics, Faculty of Pharmacy, University of Valencia, Spain.*

Received September 15, 1998. Final revised manuscript received December 30, 1998.
Accepted for publication January 8, 1999.

Abstract □ Absorption rate constants (in situ rat gut technique) and in vitro antibacterial activities of twenty fluoroquinolones have been evaluated. A biophysical model that relates the absorption of the compounds with their lipophilicity was fitted. The model considers the absorption process from the intestinal lumen as the sum of two resistances in series: aqueous diffusional barrier and lipoidal membrane. Even if partitioning into the membrane and membrane diffusion are both enhanced for lipophilic compounds, the absorption rate constant is limited by the aqueous diffusion. To estimate the influence of structural modifications on each property and to establish the role of lipophilicity in controlling in situ absorption and in vitro antibacterial activity, the PATQSAR search system is used to construct structure–property relationships. The structural models, which explain 99% of the total variance of each physicochemical property and 96% of each in vitro biological activity, provide an explicit and precise interpretation of lipophilicity, absorption, and antimicrobial activity. The results confirm the important role of lipophilicity in controlling absorption, as pointed out by the biophysical model for the piperazinyl series, and suggest the introduction of electronic factors in order to extend the model to heterologues. They also justify the mechanism by which quinolones are assumed to induce antibacterial activity.

Introduction

Absorption–lipophilicity correlations can help to explain absorption mechanisms by passive diffusion. The Plá-Delfina and Moreno absorption model¹ considers that in the small intestine diffusion can occur by two parallel paths: the aqueous pores and the lipoidal membrane. The actual absorption rate represents the sum of the rate constants governing the penetration into the lipoidal membrane and across the aqueous pores. When the molecular weight of the compounds is above approximately 250 Da, diffusion by the aqueous pathway becomes impossible, and the absorption is reduced to membrane penetration. In this case, the Higuchi-Ho equation² is able to describe in more detail the two steps involved in absorption. This equation considers that there are two resistances in series associated with the stagnant aqueous layer and the lipoidal barrier. In the present study, a lipophilicity–absorption relationship for homologous series of compounds is established by means of a previously published³ modification of the Higuchi-Ho equation, to check its utility and predictive potentialities.

In the field of computer-aided design, we have developed an interactive graphic system, PATQSAR (Population

Analysis by Topology-based QSAR), based on the topological DARC/PELCO methodology,^{4–6} for predicting physicochemical or biological properties of molecules, starting from their characteristic structural elements and the appropriate experimental data. With a view to validating the absorption–lipophilicity correlation established with the compartmental model and to gaining insight into the mechanism by which fluoroquinolones induce antimicrobial activity, we use our general QSAR search procedure to construct structure–absorption, structure–lipophilicity, and structure–activity correlations.

Materials and Methods

Test Compounds—Sixteen 6-fluoro-7-piperazinyl quinolones derived from norfloxacin and ciprofloxacin by progressive alkylation of *N*-piperazinyl,⁷ as well as four additional compounds, one homologue and three related heterologues, were provided by Cenavisa S. A. Laboratories (I+D Department, Reus, Spain).⁸

Each compound was identified by its infrared spectrum. Purity was checked by ion-pair reversed phase HPLC and shown to be above 99.9% in all cases. The names, structures, and molecular weights of the compounds are given in Table 1. The piperazinyl quinolones exhibited a pK_{a1} between 5.5 and 6.5, and a pK_{a2} between 7.5 and 8.5, and at the working pH (7.00) they were in their zwitterionic form. The heterologues have only one pK_a value between 6.0 and 7.0.

Absorption Studies—Biological Technique—The in situ rat gut technique, adapted as previously described,^{9,10} was performed using the whole small intestine of male Wistar rats weighing 210–295 g (six animals per compound). To prevent enterohepatic recycling, the bile duct was cannulated before the perfusion. An isotonic saline solution was prepared and buffered to pH 7.00 by addition of 10% (v/v) of 0.066 M Sørensen phosphate solution. This concentration prevents the disturbing effects of phosphates on the intestinal membrane¹¹ while maintaining the ionization of the substances. Test solutions were prepared immediately before use by dissolving a fixed amount of each compound in the vehicle solution (w/v), depending on its solubility. The concentrations, shown in Table 1, are low enough to avoid precipitation in the lumen during the absorption tests. After dissolving the xenobiotic, the pH of the solution was checked and readjusted when necessary. The perfusate was sampled into silanized glass tubes at fixed times after 5 min, at intervals of 5 min. All samples were analyzed immediately.

Water Reabsorption Studies—The volume of the perfused solutions at the end of the experiments was significantly reduced (up to 20%), and a correction became necessary in order to calculate the absorption rate constants accurately. If this process is not considered, the disappearance from the gut is underestimated and the absorption rate constant is incorrectly calculated. Water reabsorption is an apparent zeroth-order process.^{10,12} A method based on direct measurement of the remaining volume of the test solution was employed.⁷ The volume V_0 at the beginning of the experiment for each compound was determined on groups of three animals, while the volume V_t at each time t was measured on every animal used. The corrected concentration C_t , which represents the concentration in the gut that would exist in the absence of the water reabsorption process, was deduced from the concentration C_e analyzed in the sample at the same time t , by the following equation:

* Corresponding author: Christiane Mercier, ITODYS, 1 rue Guy de la Brosse, 75005 Paris, France. Phone: 33-1-44276803. Fax: 33-1-44276814. E-mail: mercier@itodys.jussieu.fr.

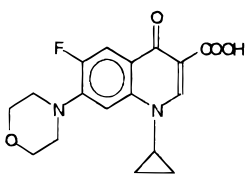
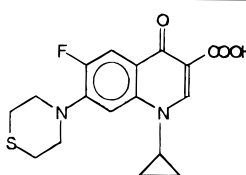
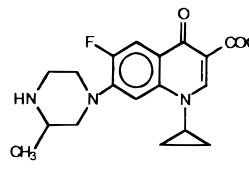
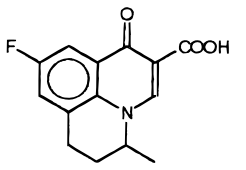
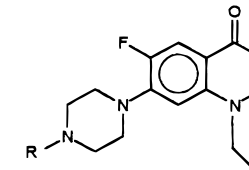
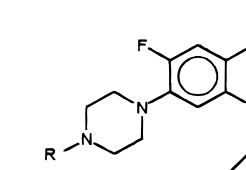
[†] The results were presented in part at the Fourth International Conference on Drug Absorption, June 13–15, 1997, Edinburgh, UK.

[‡] Department of Food Technology, Polytechnic University of Valencia, Spain.

[§] Centre d'Etudes du Bouchet, France.

^{||} ITODYS, Université Paris VII, France.

Table 1—Names, Structures, Molecular Weights and Perfusion Concentrations of Substituted 6-Fluoroquinolones

| | | | | | | | | |
|----------------------------------|---|--|-----|--|---|---|-----|---------------------------------|
| Additional 6-fluoroquinolones |  | NV 8804, 1-cyclopropyl-6-fluoro-1,4-dihydro-7-(4-morpholinyl)-4-oxo-3-quinoline carboxylic acid Perfusion concentration 50µg/mL MW=330 | |  | NV 8919, 1-cyclopropyl-6-fluoro-1,4-dihydro-7-(4-thiomorpholinyl)-4-oxo-3-quinoline carboxylic acid Perfusion concentration 11µg/mL MW=349 | | | |
| |  | CNV 97100, 1-cyclopropyl-6-fluoro-1,4-dihydro-7-(3-methyl-1-piperazinyl)-4-oxo-3-quinoline carboxylic acid Perfusion concentration 100µg/mL MW= 345 | |  | Flumequine, 9-fluoro-6,7-dihydro-5-methyl-1-oxo-1H,5H-pyrido[3,2,1-ij]quinoline-2-carboxylic acid Perfusion concentration 100µg/mL MW= 261 | | | |
| 6-fluoro-7-piperazinylquinolones |  | R | MW | Perfusion concentration (µg/mL) |  | R | MW | Perfusion concentration (µg/mL) |
| | H- | Norflloxacin, 1-ethyl-1,4-dihydro-4-oxo-6-fluoro-7-(N-piperazinyl)-3-quinoline carboxylic acid | 319 | 100 | H- | Ciprofloxacin, 1-cyclopropyl-1,4-dihydro-4-oxo-6-fluoro-7-(N-piperazinyl)-3-quinoline carboxylic acid | 331 | 100 |
| | CH ₃ - | N'-methylnorflloxacin | 333 | 100 | CH ₃ - | N'-methylciprofloxacin | 345 | 100 |
| | CH ₃ -CH ₂ - | N'-ethylnorflloxacin | 347 | 100 | CH ₃ -CH ₂ - | N'-ethylciprofloxacin | 359 | 100 |
| | CH ₃ -(CH ₂) ₂ - | N'-propylnorflloxacin | 361 | 100 | CH ₃ -(CH ₂) ₂ - | N'-propylciprofloxacin | 373 | 100 |
| | CH ₃ -(CH ₂) ₃ - | N'-butylnorflloxacin | 375 | 100 | CH ₃ -(CH ₂) ₃ - | N'-butylciprofloxacin | 387 | 80 |
| | CH ₃ -(CH ₂) ₄ - | N'-pentylnorflloxacin | 389 | 50 | CH ₃ -(CH ₂) ₄ - | N'-pentylciprofloxacin | 401 | 50 |
| | CH ₃ -(CH ₂) ₅ - | N'-hexylnorflloxacin | 403 | 25 | CH ₃ -(CH ₂) ₅ - | N'-hexylciprofloxacin | 415 | 40 |
| | CH ₃ -(CH ₂) ₆ - | N'-heptylnorflloxacin | 417 | 6 | CH ₃ -(CH ₂) ₆ - | N'-heptylciprofloxacin | 429 | 6 |

$$C_t = C_e \frac{V_t}{V_0} \quad (\text{eq 1})$$

Absorption Rate Constants—The absorption rate constants k_a were determined by nonlinear regression analysis of the corrected concentrations C_t versus time, using Sigma Plot 2.0 (Jandel Scientific), as it had been previously established that the process follows first-order kinetics. To prevent adsorption on the intestinal mucosa and residual sample dilution effects,^{10,13} only the calculated values after 5 min, listed in Table 2, were used for regression, as it was found that after that time adsorption equilibrium was generally reached.

Lipophilicity Indexes—*Partition Coefficients*—Bulk phase partition coefficients, P , between *n*-octanol (Merck analytical grade) and of 0.066 M Sørensen phosphate buffer, pH 7.00, were determined for each compound of the series. Six values per compound were used to establish the average value to be used in the correlations. These values are reported in previous papers.^{3,14}

Number of Methylene Groups—This was used as a lipophilicity index free of the influence of solvent interactions. Provided that a

perfect homologous series is studied, it has been demonstrated to be equivalent to other indexes such as partition coefficients, P ,^{1,15} or capacity factors, K .

Analysis of the Samples—An original HPLC procedure was used to quantify the solute concentration in both biological and partition samples. The analysis was carried out on a Novapak C18 column (3.9 × 150 mm), using as mobile phase a mixture of methanol and 15 mM phosphate buffer, adjusted to pH 2.4 with orthophosphoric acid. The percentage of each component of the mobile phase was selected for each compound of the series in order to obtain the best chromatographic resolution. The equipment consisted of a Series III Hewlett-Packard quaternary pump, a Rheodyne injector, a 1046 Hewlett-Packard fluorescence detector, and a 3395 Hewlett-Packard integrator. Quantification was done by fluorometry, with excitation and emission wavelengths of 338 and 425 nm, respectively. This technique offers a high degree of selectivity and specificity. The procedure was validated for inter- and intraday runs before use. Accuracy was estimated from the percentage error associated with measuring 5 to 8 standards, analyzed at least three times. Accuracy was demonstrated to be

Table 2—Observed and Calculated Partition Coefficients, Absorption Rate Constants, and in Vitro Antibacterial Activities

| compound | <i>P</i> | log <i>P</i> | | <i>k_a</i> (h ⁻¹) | log <i>k_a</i> | | log 1/MIC <i>E. coli</i> | | log 1/MIC <i>Staph.</i> | |
|-------------------------------|----------------------|---------------------------|------------|---|---------------------------|------------|--------------------------|------------|-------------------------|------------|
| | | obsd | calcd eq 3 | | obsd | calcd eq 4 | obsd | calcd eq 5 | obsd | calcd eq 6 |
| norfloxacin | 0.03 ^b | -1.55 (0.03) ^b | -1.60 | 0.42 ^b | -0.38 (0.07) ^b | -0.32 | 1.00 ^b | 1.03 | 0.30 | 0.33 |
| <i>N</i> -methylnorfloxacin | 1.88 ^b | 0.27 (0.01) ^b | 0.22 | 1.92 ^b | 0.28 (0.04) ^b | 0.32 | 1.00 ^b | 1.03 | 0.30 | 0.33 |
| <i>N</i> -ethylnorfloxacin | 2.36 ^b | 0.37 (0.01) ^b | 0.48 | 2.75 ^b | 0.44 (0.03) ^b | 0.46 | 0.70 ^b | 0.75 | 0.30 | 0.33 |
| <i>N</i> -propylnorfloxacin | 11.28 ^b | 1.05 (0.01) ^b | 1.01 | 4.07 ^b | 0.61 (0.04) ^b | 0.60 | 0.40 ^b | 0.47 | 0.00 | 0.05 |
| <i>N</i> -butylnorfloxacin | 30.34 ^b | 1.48 (0.02) ^b | 1.54 | 5.59 ^b | 0.75 (0.02) ^b | 0.74 | 0.40 ^b | 0.20 | -0.30 | -0.23 |
| <i>N</i> -pentylnorfloxacin | 127.67 ^b | 2.11 (0.02) ^b | 2.08 | 5.69 ^b | 0.76 (0.04) ^b | 0.74 | 0.40 ^b | 0.20 | -0.30 | -0.51 |
| <i>N</i> -hexylnorfloxacin | 515.95 ^b | 2.71 (0.01) ^b | 2.61 | 5.98 ^b | 0.78 (0.05) ^b | 0.74 | -0.20 ^b | -0.08 | -0.60 | -0.80 |
| <i>N</i> -heptylnorfloxacin | 1664.69 ^c | 3.22 (0.02) ^b | 3.14 | 6.00 ^b | 0.78 (0.04) ^b | 0.74 | -0.51 ^b | -0.35 | -1.20 | -1.07 |
| ciprofloxacin | 0.08 ^c | -1.12 (0.02) ^c | -1.07 | 0.63 | -0.20 (0.06) | -0.26 | 1.60 | 1.58 | 0.60 | 0.61 |
| <i>N</i> -methylciprofloxacin | 1.42 ^c | 0.15 (0.06) ^c | 0.22 | 2.55 | 0.41 (0.04) | 0.38 | 1.60 | 1.58 | 0.60 | 0.61 |
| <i>N</i> -ethylciprofloxacin | 3.38 ^c | 0.53 (0.01) ^c | 0.48 | 3.52 | 0.55 (0.03) | 0.52 | 1.30 | 1.30 | 0.60 | 0.61 |
| <i>N</i> -propylciprofloxacin | 11.86 ^c | 1.07 (0.01) ^c | 1.01 | 4.79 | 0.68 (0.05) | 0.66 | 1.00 | 1.03 | 0.30 | 0.33 |
| <i>N</i> -butylciprofloxacin | 35.30 ^c | 1.55 (0.04) ^c | 1.54 | 5.69 | 0.76 (0.03) | 0.80 | 0.70 | 0.75 | 0.30 | 0.05 |
| <i>N</i> -pentylciprofloxacin | 116.04 ^c | 2.06 (0.01) ^c | 2.07 | 6.04 | 0.78 (0.02) | 0.80 | 0.70 | 0.75 | -0.30 | -0.23 |
| <i>N</i> -hexylciprofloxacin | 361.71 ^c | 2.56 (0.02) ^c | 2.61 | 6.03 | 0.78 (0.04) | 0.80 | 0.40 | 0.47 | -0.60 | -0.51 |
| <i>N</i> -heptylciprofloxacin | 1043.96 ^c | 3.02 (0.04) ^c | 3.14 | 6.08 | 0.78 (0.04) | 0.80 | 0.40 | 0.20 | -0.90 | -0.80 |
| CNV8919 | 54.71 | 1.74 (0.02) | 1.76 | 7.52 | 0.88 (0.03) | 0.87 | | | | |
| flumequine | 9.38 | 0.97 (0.02) | 0.96 | 6.87 | 0.84 (0.04) | 0.82 | | | | |
| CNV97100 | 0.09 | -1.07 (0.06) | -1.07 | 1.24 | 0.09 (0.07) | 0.09 | | | | |
| CNV8804 | 9.37 | 0.97 (0.01) | 0.96 | 7.10 | 0.85 (0.06) | 0.87 | | | | |
| mean SD ^a | | (0.02) | | | (0.04) | | | | | |

^a SD: standard deviation. ^b Data from ref 3. ^c Data from ref 14.

better than 15%, regardless of the analyte concentration. Precision was calculated as the coefficient of variation of five determinations over the same standards, and it was shown to be better than 5%. Linearity was established over the range of concentrations present in the samples for every compound (correlation coefficients always over 0.999).

In Vitro Antibacterial Activity—The lowest concentration of the drug that inhibited the growth of 90% of the strains on agar was taken as the minimum inhibitory concentration, MIC₉₀. It was determined on 100 strains of *Escherichia coli*, using the agar plate dilution method. The procedure was validated by means of the following typified strains: *Pseudomonas aeruginosa* ATCC 27853, *E. coli* ATCC 25922, *Streptococcus faecalis* ATCC 29212, and *Staphylococcus aureus* ATCC 29213. The assay was carried out following the specifications of the National Committee for Clinical Laboratory Standards.¹⁶ Mueller-Hinton agar plates were prepared with known concentrations of the quinolone tested, covering a suitable range. The bacterial suspension was then inoculated into the plates with a Steers replicator. The plates were cultured at 37 °C for 20 h and evaluated immediately thereafter.

Fitting of Models to the Data—To test the pertinence of the absorption rate constants for establishing correlations, their values were compared with each of those by means of ANOVA after the homogeneity of the variance had been tested using the Cochran test.

Absorption—Lipophilicity Relationship—A biophysical compartmental model, which considers the total resistance to passive absorption as the sum of two resistances in series, was fitted. As previously pointed out,³ the partial resistances correspond to the aqueous resistance, produced by the stagnant aqueous layer and to the lipoidal resistance due to the membrane. The original equation^{2,3,17} was adapted assuming that the permeability in the aqueous layer depends inversely on the square root of the molecular weight and that the permeability in the membrane lipoidal phase is related to lipophilicity. The equation can be written as follows:

$$k_a = \frac{CP^d}{1 + E\sqrt{MP^d}} \quad (\text{eq 2})$$

where *C*, *d*, and *E* are fitting parameters. Curve fitting was carried out only for perfectly homologous compounds. All fitting operations were run on a computer using the PCNONLIN 4.0 program. For more complicated fitting models, PCNONLIN was used instead of Sigma Plot because it is a more powerful software which uses several algorithms to optimize the objective function, provides more statistical information about the parameters obtained, and gives the standard deviation of the predicted values. To appreciate the goodness of fit, the correlation coefficients between the experimental and model-predicted *k_a* values were calculated. Precision in the estimation of the parameters, and the standard deviation, *s*, were also used as criteria for evaluating the results.

Structural Models—Four correlations were run on the compounds and the available data for each property. The experimental population consisted of 20 compounds for the absorption rate and partition coefficients, and 16 for in vitro antibacterial activity. The models were established by using PATQSAR,¹⁸ a system for QSAR search based on the DARC/PELCO topological procedure.⁴⁻⁶

Data are encoded directly by an interactive procedure. The compounds are represented as ordered chromatic graphs. Their superposition generates the population trace, which contains all the elements required for constructing the initial structural variable automatically. Compounds are described by a vector of discrete structural variables, which have values of 0 or 1 depending on their absence from or presence in the molecule, respectively.

These primary variables can be further combined into more complex ones:

Interaction variables designate the simultaneous existence of two or more basic structural elements, each of which can exist without the other; they are written as $V_1 * V_2$;

Exclusion variables designate the existence of a basic element in the absence of another one, which can exist simultaneously; they are represented as $V_1 * \bar{V}_2$;

Equivalence variables make elements, which belong to homogeneous series and have closely similar effects on the property, equivalent; they are written as $V_1 = V_2$.

Optimal correlations were sought on the basis of the criterion of experimental precision (± 0.04 for log *k_a* and ± 0.02 for log *P*). For each model an exploratory correlation was run on the available data with all the topochromatic "sites" as parameters, i.e., atoms and bonds different from the common structure or "focus". Deviations from additivity were taken into account by introducing interaction sites. Regularities, which allow certain structural effects to be generalized, were detected by introducing equivalence sites. At each step the new SAR is set up by multiple linear regression analysis. A stepwise module is available to detect the most significant parameters.

Results and Discussion

Lipophilicity Indexes—The *n*-octanol/water partition coefficients listed in Table 2 undoubtedly constitute the most classic index. To study the effect of alkylation on lipophilicity, the relationships between log *P* and the number of methyl groups of homologous compounds were established for each series. Statistical comparison (*t* test) of their slopes demonstrated that they are the same. Therefore, the overall correlation is shown in Figure 1. In such a correlation the intercept should represent the log *P* value of the parent compounds of the series (i.e. norfloxacin and ciprofloxacin), but it does not. This can be interpreted as the result of specific interactions between these elements and the solvent, promoted by the absence of the methyl substituent. This effect has been reported for many parent

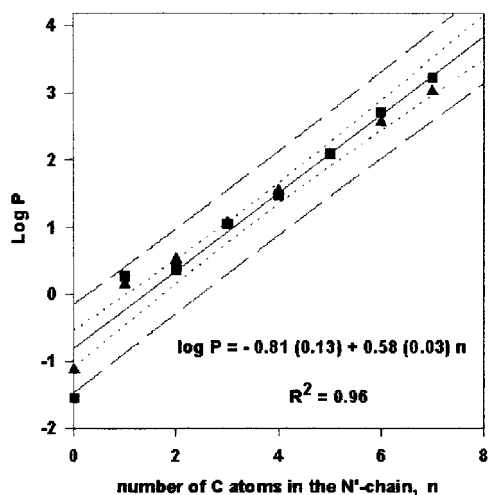


Figure 1—Relationship between partition coefficient and number of methylene groups for *N*-alkylnorfloxacin (■) and *N*-alkylciprofloxacin (▲). The dotted and dashed lines represent the 95% confidence (···) and prediction (---) intervals, respectively.

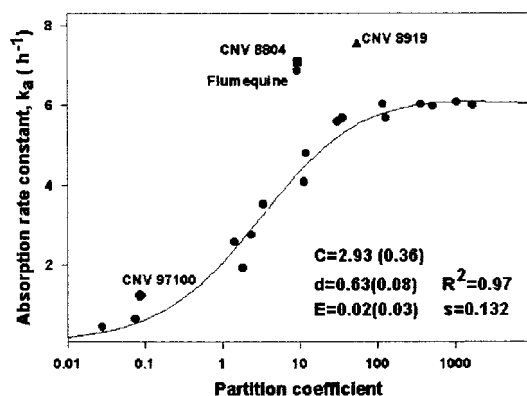


Figure 2—Relationship between absorption and partition coefficient for perfectly homologous compounds. The line represents the best fit of eq 2: $k_a = (2.60P^{0.72})/(1 + 0.02P^{0.72})$. The points associated with the heterologues are superimposed: CNV 8804 (■); CNV 8919 (▲); flumequine (●).

compounds of very different homologous series. The methyl derivatives, on the contrary, show higher lipophilicity indexes than predicted. This effect, known as the “first element effect”, can easily be explained if we consider the fact that the methyl group has a larger volume than the hydrogen of the parent ring. Therefore, the substituent significantly reduces the water to *n*-octanol transfer energy. Obviously, this substituent produces greater changes than subsequent alkylation. Finally, the slope of the correlation, which represents $\Delta\pi$ for the series, is in good agreement with Hansch's predictions.

Absorption–Lipophilicity Correlation—Applying the biophysical model to the 17 6-fluoro-7-piperazinylquinolones leads to a very significant absorption–lipophilicity correlation ($R^2 = 0.97$) represented in Figure 2 where the fitting parameters are listed along with the statistical data. As can be seen, the absorption rate constant increases with lipophilicity up to a certain value because of the limiting effect of water diffusion through the stagnant layer. Therefore, there is a practical limit to the lipophilicity that improves the intestinal absorption rate. The k_a and P values of the three heterologous compounds have also been plotted in Figure 2. Their absorption rate constants are higher than those predicted by the correlation from their lipophilicity index. This could be due to the electronic changes that the new substituents introduce into the molecule, which probably modify their interactions with the absorptive membrane. Nevertheless, the optimal values

for lipophilicity that could be predicted reproduce the value obtained by the correlation for homologous compounds.

Structural Models—Lipophilicity–Structure Model—The results are displayed on the population trace diagram in Table 3. The relationship can be written:

$$\log P = 0.96 (\pm 0.04) \text{N} - 2.56 (\pm 0.05) \text{N} + 0.81 (\pm 0.03) \text{S} + 1.82 (\pm 0.05) C_1 + 0.27 (\pm 0.01) C_2 + 0.54 (\pm 0.02) \sum_{i=3}^7 C_i + 0.54 (\pm 0.02) \text{CH}_2 * \bar{C}_1$$

$$R^2 = 0.99 \quad F = 2556 \quad s = 0.07 \quad df = 16 \quad n = 20 \quad (\text{eq. 3})$$

where:

ΣC_i groups the chain-lengthening atoms; $\text{CH}_2 * \bar{C}_1$ represents the methylene bridge in the absence of chain-lengthening on the piperazinyl ring; the contribution of the methylene bridge is zero when C_1 is present.

The structural elements, whose contributions are 0.27, 0.54, and 0.81, are grouped in an equivalence variable where they are weighted as indicated below:

$$C_2 = 1, \quad C_3 = C_4 = C_5 = C_6 = C_7 = \text{CH}_2 * \bar{C}_1 = 2, \quad \text{S} = 3$$

Contributions of the different heterocycles take into account the absence of the flumequine moiety represented by the dotted line in Table 3.

The lipophilicity, as expected, is markedly reduced by introducing a piperazinyl ring at position 7. Replacing the *N'* nitrogen of this ring by a different heteroatom, oxygen or sulfur, produces a more lipophilic molecule. The lipophilicity is decreased by a higher electron-donating effect of the substituent which enhances its solvation by water. It is greatly increased upon methylation of the *N*-piperazinyl nitrogen (+1.82) and regularly enhanced by lengthening or branching of the *N*-alkyl chains (+0.54) except in the β positions with respect to the *N'* nitrogen. The contribution of the first methyl to total lipophilicity is about three times that of the chain-lengthening atoms. This can be explained by the fact that secondary amines have a higher polarity and affinity for the aqueous phase and interact with it more easily. Replacing the hydrogen by a donor substituent, such as the methyl group, reduces the transfer energy from water into *n*-octanol.¹⁹ The small contribution of the β chain-lengthening atom (0.27) compensates the first element effect. Replacing the *N*-ethyl by a *N*-cyclopropyl in position 1 increases lipophilicity by the same 0.54 value but has no effect in the presence of a *N'*-chain. The influence of the methylene bridge is quantified by the interaction–exclusion variable. Surprisingly, introducing a methyl group on the piperazinyl ring at the β position with respect to the *N'* nitrogen has no effect.

Absorption–Structure Model. The relationship presented in Table 4 can be expressed as:

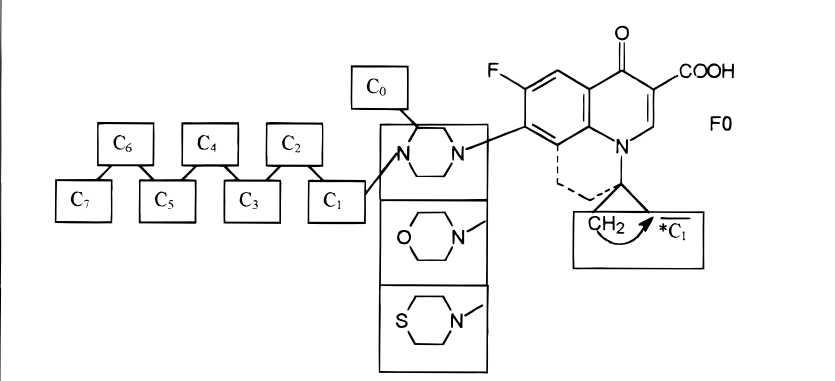
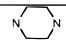

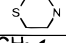
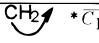
$$\log k_a = 0.82 (\pm 0.02) - 1.13 (\pm 0.03) \text{N} + 0.06 (\pm 0.02) \text{CH}_2 + 0.35 (\pm 0.04) C_0 + 0.64 (\pm 0.03) C_1 + 0.14 (\pm 0.01) \sum_{i=2}^4 C_i$$

$$R^2 = 0.99 \quad F = 387 \quad s = 0.04 \quad df = 14 \quad n = 20 \quad (\text{eq. 4})$$

In this case the interaction variable is not necessary because the membrane behaves as a less discriminative partitioning system than *n*-octanol/water.

The 7-piperazinyl group reduces both lipophilicity and absorption, as this implies an increase in polarity.¹⁹ Again, replacing the nitrogen of the piperazinyl ring by a different heteroatom, oxygen or sulfur, enhances both lipophilicity

Table 3—Structure–Lipophilicity Model

| Structural elements | Lipophilicity contributions | Structural elements | Lipophilicity contributions |
|--|-----------------------------|---------------------|-----------------------------|
|  | 0.96 (± 0.04) | C ₀ | 0.00 |
|  | 2.56 ^a (± 0.05) | C ₁ | 1.81 (± 0.05) |
|  | 0.00 ^a | C ₂ | 0.27 (± 0.01) |
|  | 0.81 ^a (± 0.03) | C ₃ | 0.54 (± 0.02) |
|  | 0.54 ^b (± 0.02) | C ₄ | 0.54 (± 0.02) |
| | | C ₅ | 0.54 (± 0.02) |
| | | C ₆ | 0.54 (± 0.02) |
| | | C ₇ | 0.54 (± 0.02) |

^a Contributions of the heterocyclic rings take into account the absence of the flumequine moiety represented by the dashed line. ^b Contribution of the methylene bridge is zero when C₁ is present.

and absorption. However, the relative contributions are not the same. Starting from flumequine whose lipophilicity is a little higher than absorption, introducing the 7-piperazinyl group decreases lipophilicity (−2.56) much more than absorption (−1.13) while introducing a morpholinyl or a thiopiperidyl group either has no effect on both properties or increases lipophilicity (+0.81) markedly and does not influence absorption. Introducing a methylene bridge into the *N*-ethyl side chain strengthens this effect, leading to heterologues having a higher lipophilicity than absorption, in contrast to the first terms of the piperazinyl series. This could explain why they were found as outliers in the biophysical model. It suggests that absorption is an increasing function of lipophilicity which must be modulated by electronic factors.

In the piperazinylquinolones, each chain-lengthening atom that increases lipophilicity produces an increase in absorption up to four carbons. The relative contributions are also reproduced: the first methyl group produces a bigger increase than any other, as previously seen for log *P*, and further elongation produces a uniform absorption increase. However, in this case the scheme changes, the three last chain-lengthening atoms have no effect on absorption and can be ignored. This fact can be understood if we consider the biophysical model. As stated by Higuchi-Ho, adjacent to the intestinal membrane there is an aqueous diffusion barrier, whose thickness creates an aqueous resistance to solute diffusion which has to be overcome before partitioning into the membrane. This step represents the absorption rate-limiting process. Even if partitioning into the membrane and membrane diffusion are enhanced for lipophilic compounds, the absorption rate has

a practical limit fixed by the aqueous diffusion,³ as is clear from the zero contribution of the three last chain-lengthening elements.

Additionally, introducing a 3'-methyl group or a 1-cyclopropyl has a slightly different effect on absorption and lipophilicity: 3'-methyl, which has no influence on lipophilicity, increases absorption weakly; 1-cyclopropyl, which has no influence on absorption, increases lipophilicity but only for the first term.

Structure–Antibacterial Activity Models—The results are displayed on the population trace diagrams in Tables 5 and 6. The equations can be written:

$$\log(1/MIC)_{E.Coli} = 1.03 (\pm 0.03) - 0.28 (\pm 0.01) \sum_{i=2}^7 C_i + 0.56 (\pm 0.02) \text{CH}_2$$

$$R^2 = 0.96 \quad F = 371 \quad s = 0.11 \quad df = 14 \quad n = 16 \quad (\text{eq. 5})$$

The two structural elements are grouped in an equivalence variable, where they are weighted as indicated:

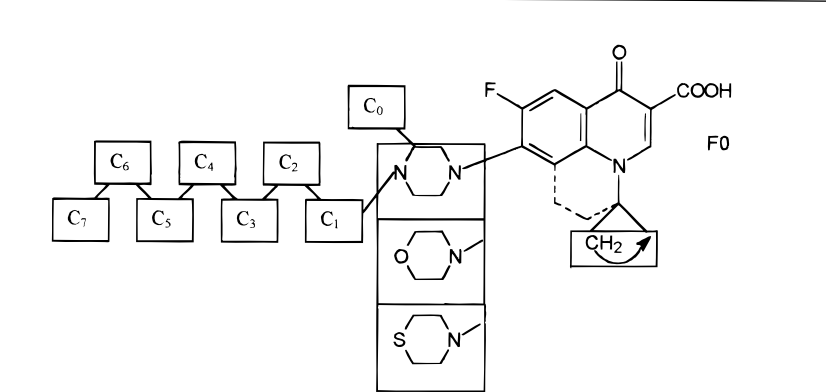
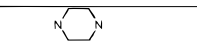
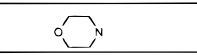
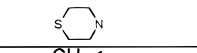

$$C_2 = C_3 = C_4 = C_5 = C_7 = -1, \quad \text{CH}_2 = 2.$$

$$\log(1/MIC)_{Staph.} = 0.33 (\pm 0.04) - 0.28 (\pm 0.02) \sum_{i=3}^7 C_i + 0.28 (\pm 0.02) \text{CH}_2$$

$$R^2 = 0.96 \quad F = 323 \quad s = 0.12 \quad df = 14 \quad n = 16 \quad (\text{eq. 6})$$

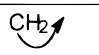
In this case, the two structural elements grouped in the equivalence variable are weighted:

Table 4—Structure–Absorption Model

| Structural elements | Absorption contributions | Structural elements | Absorption contributions |
|--|------------------------------|---------------------|--------------------------|
|  | 0.82 (± 0.02) | C ₀ | 0.35 (± 0.05) |
| | | C ₁ | 0.64 (± 0.03) |
| | | C ₂ | 0.14 (± 0.01) |
| | | C ₃ | 0.14 (± 0.01) |
|  | - 1.13 ^a (± 0.05) | C ₄ | 0.14 (± 0.01) |
|  | 0.00 ^a | C ₅ | 0.00 |
|  | 0.00 ^a | C ₆ | 0.00 |
|  | 0.06 (± 0.02) | C ₇ | 0.00 |

^a Contributions of the heterocyclic rings take into account the absence of the flumequine moiety represented by the dashed line.

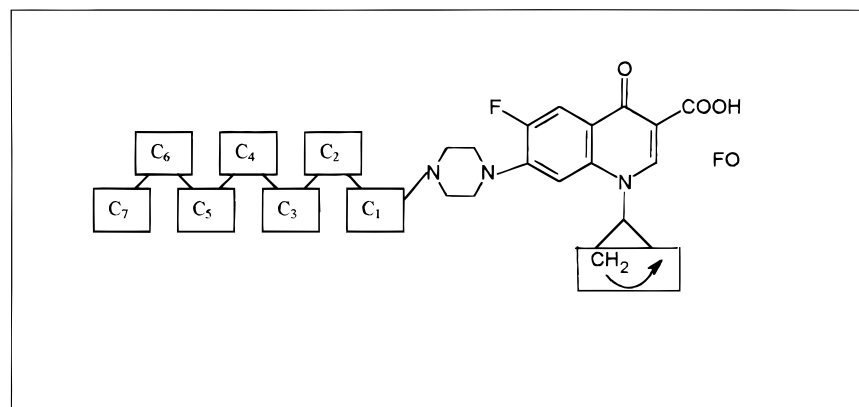
Table 5—Structure–Antibacterial Activity Model for *Escherichia coli*

| FO | | 1.03 (± 0.03) | |
|----------------|-----------------|---|-----------------|
| C ₁ | 0.00 | C ₅ | - 0.28 (± 0.01) |
| C ₂ | - 0.28 (± 0.01) | C ₆ | 0.00 |
| C ₃ | - 0.28 (± 0.01) | C ₇ | - 0.28 (± 0.01) |
| C ₄ | - 0.28 (± 0.01) |  | 0.56 (± 0.02) |

$$C_3 = C_4 = C_5 = C_6 = C_7 = -1, \text{CH}_2 = 1$$

As can be observed, only replacing the ethyl by a

cyclopropyl substituent enhances the antimicrobial activity. This effect has been reported previously.^{19,20} Nevertheless, in these studies the step concerned in the mechanism, either the cellular penetration or an interaction between

Table 6—Structure–Antibacterial Activity Model for *Staphylococcus aureus*


| | | | |
|----------------|-----------------|-----------------|-----------------|
| FO | | 0.33 (± 0.04) | |
| C ₁ | 0.00 | C ₅ | - 0.28 (± 0.02) |
| C ₂ | 0.00 | C ₆ | - 0.28 (± 0.02) |
| C ₃ | - 0.28 (± 0.02) | C ₇ | - 0.28 (± 0.02) |
| C ₄ | - 0.28 (± 0.02) | CH ₂ | 0.28 (± 0.02) |

the cyclopropyl group and the DNA or bacterial girase binding site, was not clarified. On the other hand, it can be noted that the activity on both strains is decreased by lengthening the *N*-alkyl chain. According to the structure–lipophilicity model, these structural effects are not related to cellular penetration, as the methylene bridge has no influence on lipophilicity, and chain-lengthening increases it. Thus, antibacterial activity is enhanced by a *N*-cyclopropyl which could help to bind the molecule to the DNA or to the bacterial girase. It is decreased by steric hindrance of the *N*-alkyl chain which could hinder access of the molecule to the enzyme or its intercalation in the DNA.

Conclusion

Two strategies are used to identify the properties which influence in situ absorption. In the first, the influence is assessed quantitatively by searching for correlations between absorption and lipophilicity. Within the series of closely related piperazinyl fluoroquinolones, lipophilicity appears as a strong determinant factor, and the results validate our previous biophysical model. Although the three heterologues are found as outliers, the biophysical model is still able to predict the lowest value of lipophilicity for a maximum absorption. In the second strategy, we construct structural models by using the PATQSAR approach and deduce the influence, starting from a simultaneous analysis of absorption and lipophilicity. The results confirm that absorption is increased by higher lipophilicity up to a limit due to *N*-chain lengthening which could hinder membrane penetration by steric hindrance. Moreover, they suggest that electronic factors could be introduced into the biophysical model in order to reflect the marginal behavior of the heterologues.

The PATQSAR approach confirms some of the hypotheses of the biophysical absorption model and suggests its extension, thus demonstrating that they are complementary. Moreover, its use to identify the properties which influence antibacterial activity suggests the role of steric

factors. This system is therefore a powerful tool for interpreting physicochemical and biological data and for optimizing certain processes, such as in situ absorption and antibacterial activity.

References and Notes

- Plá-Delfina, J. M.; Moreno, J. Intestinal absorption-partition relationship: a tentative functional nonlinear model. *J. Pharmacokin. Biopharm.* **1981**, *9*, 191–215.
- Suzuki, A.; Higuchi, W. I.; Ho, N. F. H. Theoretical model studies of drug absorption and transport in the gastrointestinal tract. II. *J. Pharm. Sci.* **1970**, *59*, 644–651.
- Merino, V.; Freixas, J.; Bermejo, M. V.; Garrigues, T. M.; Moreno, J.; Plá Delfina, J. M. Biophysical models as an approach to study passive absorption in drug development: 6-fluoroquinolones. *J. Pharm. Sci.* **1995**, *84*, 777–782.
- Sobel, Y.; Vizet, P.; Chemob, S.; Barbieux, F.; Mercier, C. Enhancing the flexibility and adaptability of the DARC structural representation for computer-aided Drug Design. *SAR and QSAR in Environ. Res.* **1998**, *9*, 83–109.
- Mercier, C.; Sobel, Y.; and Dubois, J. E. DARC/PELCO method: a topological tool for QSAR search and its reliable predictive capability. In *Chemical Graph Theory*; Bonchev, D., Rouvray, D. H., Eds.; Gordon and Breach: Philadelphia, 1992, pp 199–257.
- Mercier, C.; Fabart, V.; Sobel, Y.; Dubois, J. E. Modeling alcohol metabolism with the DARC/CALPHI system. *J. Med. Chem.* **1991**, *34*, 934–942.
- Koga, H. Structure–activity relationships of antibacterial 6,7- and 7,8-disubstituted 1-alkyl-1,4-dihydro-4-oxoquinoline-3-carboxylic acids. *J. Med. Chem.* **1980**, *23*, 1358–1363.
- Cenavisa, S. A. Spanish Patent 8,901,480, 1989.
- Doluisio, J. T.; Billups, N. F.; Dittert, L. W.; Sugita, E. T.; Swintosky, J. V. Drug absorption. I. An in situ rat gut technique yielding realistic absorption rates. *J. Pharm. Sci.* **1969**, *58*, 1196–1199.
- Martín-Villodre, A.; Plá-Delfina, J. M.; Moreno, J.; Pérez-Buendía, M. D.; Miralles-Mir, J.; Collado, E. F.; Sánchez-Moyano, E.; Del Pozo, A. Studies on the reliability of a bihyperbolic functional absorption model. I. Ring substituted anilines. *J. Pharmacokin. Biopharm.* **1986**, *14*, 615–633.
- Morishita, T.; Yamazaki, M.; Yata, N.; Kamada, A. Studies on absorption of drugs. Physicochemical factors affecting the absorption of sulfonamides from the rat small intestine. *Chem. Pharm. Bull.* **1973**, *21*, 2309–2322.

12. Gabus-Sannié, C.; Buri, P. Étude comparative des méthodes de détermination du volume d'eau absorbé lors de la perfusion de l'intestin grêle du rat. *S. T. P. Pharma* **1987**, *3*, 856–860.
13. Doluisio, J. T.; Crouthamel, W. G.; Tan, G. H.; Swintosky, J. V.; Dittert, L. W. Drug absorption. III. Effect of membrane storage on the kinetics of drug absorption. *J. Pharm. Sci.* **1970**, *59*, 72–76.
14. Merino, V.; Martín-Algarra, R.; Rocher, A.; Garrigues, T. M.; Freixas, J.; Polache, A. Effects of ethanol on intestinal absorption of drugs I. In situ studies with ciprofloxacin analogues in normal and chronic alcohol fed rats. *Alcohol Clin. Exp. Res.* **1997**, *41*, 1996–2000.
15. Plá-Delfina, J. M.; Pérez Buendía, J. M.; Casabó, V. G.; Peris Ribera, J. E.; Martín Villodre, A. Absorption-partition relationships for true homologous series of compounds as a possible approach to study mechanism of surfactants in absorption. I. Aromatic amines in rat colon. *Int. J. Pharm.* **1987**, *37*, 49–64.
16. NCCLS Document M 100-S, Vol. 6, No. 21. National Committee for Clinical Laboratory Standards (NCCLS): Villanova, Philadelphia, 1986.
17. Ho, N. F. H.; Park, J. Y.; Morozowich, W.; Higuchi, W. I. Physical model approach to the design of drugs with improved intestinal absorption. In *Design of Biopharmaceutical Properties through Prodrugs and Analogues*; American Pharmaceutical Association: Washington, D.C., 1977; pp 136–227.
18. Vizet, P. PATQSAR, version 2.55, **1997**.
19. Takacs-Novak, K.; Jozan, M.; Hermecz, I.; Szasz, G. Lipophilicity of antibacterial fluoroquinolones. *Int. J. Pharm.* **1992**, *79*, 89–96.
20. Bryskier, A.; Chantot, J. F. Classification and structure–activity relationships of fluoroquinolones. *Drugs* **1995**, *49*, 16–28.
21. Wolfson, J. S.; Hoopert, D. Pharmacokinetics of quinolones: newer aspects of antimicrobial agents. *Chemotherapy* **1985**, *28*, 581–586.

Acknowledgments

The present work is a part of a research project carried out with a grant from CICYT (SAF96-1710) from the Education and Science Ministry (Spain) and from the Defense Ministry (France). The authors are indebted to the Education, Culture and Science Department of Valencian Generalitat for a grant (Marival Bermejo). The authors are also indebted to Mr. J. Freixas of Cenavisa for supplying the compounds studied and some of the MIC data.

JS980370+